Catal Lett (2007) 118:203–210
DOI 10.1007/s10562-007-9163-0

Characterization of Supported $NiSO_4$ and Effect of TiO_2–ZrO_2 Composition on Catalytic Activity for Acid Catalysis

Jong Rack Sohn · Si Hoon Lee

Received: 14 February 2007 / Accepted: 11 June 2007 / Published online: 11 July 2007

Abstract A series of catalysts, $NiSO_4/TiO_2$–ZrO_2 having different TiO_2–ZrO_2 composition, for acid catalysis was prepared by the impregnation method using an aqueous solution of nickel sulfate. The addition of TiO_2 to ZrO_2 improved the surface area of the catalyst and enhanced its acidity remarkably because of the formation of new acid sites through the charge imbalance of Ti–O–Zr bonding. The binary oxide, TiO_2–ZrO_2 calcined above 600 °C resulted in the formation of crystalline orthorhombic phase of $ZrTiO_4$. Therefore, $NiSO_4/TiO_2$–ZrO_2 calcined at 500 °C exhibited a maximum catalytic activity for acid catalysis, and then the catalytic activity decreased with the calcination temperature. The correlation between catalytic activity and acidity held for both reaction, 2-propanol dehydration and cumene dealkylation. $NiSO_4$ supported on $50TiO_2$–$50ZrO_2$ (TiO_2/ZrO_2 ratio = 1) among TiO_2–ZrO_2 binary oxides exhibited the highest catalytic activity for acid catalysis.

Keywords $NiSO_4/TiO_2$–ZrO_2 · Acidity · TiO_2–ZrO_2 composition · $ZrTiO_4$ phase · Cumene dealkylation · 2-Propanol dehydration

1 Introduction

Acid catalysis is of fundamental industrial importance. It plays a vital role in many important reactions of the chemical and petroleum industries, and environmentally benign chemical processes [1–3]. The use of liquid phase superacid catalysts presents serious problems: It is difficult to separate the acid and the product stream, large amount of catalyst is usually required, and the catalyst waste is significant, causing an environmental hazard. Furthermore, the cost of process installation and maintenance is high since the liquid acids are very corrosive. It has been sought for long to replace liquid acid for solid showing comparable catalytic properties [1]. Strongly acidic sites can be created within the pores of some high silica zeolites, but, over zeolite catalysts the conversion of paraffins into branched products is low due to steric constraints. Liquid superacids based on HF, which are efficient and extensively used in catalytic processing, are not suitable for industrial processes due to separation problems tied with environmental regulations [4]. Thus the search for environmentally benign heterogeneous catalysts has driven the worldwide research of new materials as a substitute for current liquid acids and halogen-based solid acids. Among them sulfated oxides, such as sulfated zirconia, titania, and iron oxide exhibiting high thermostability, superacidic property, and high catalytic activity, have evoked increasing interest [1, 2, 5]. The strong acidity of zirconia-supported sulfate has attracted much attention because of its ability to catalyze many reactions such as cracking, alkylation, and isomerization.

A number of combination of metal oxides generates acid sites [6–13]. Binary metal oxides are expected to exhibit better catalytic activity for some reactions due to their solid acid or base properties [14]. Among various binary oxides, the TiO_2–ZrO_2 exhibited very good catalytic activity. The TiO_2–ZrO_2 binary oxide has also been reported to exhibit high surface acidity by a charge imbalance based on the generation of Ti–O–Zr bonding [15]. Further, recent studies also reveal that TiO_2–ZrO_2 is an active catalyst for

J. R. Sohn (✉)
Department of Applied Chemistry, Engineering College, Kyungpook National University, Taegu 702-701, Korea
e-mail: jrsohn@knu.ac.kr

S. H. Lee
Environment Research Team, Research Institute of Industrial Science and Technology, Pohang 790-330, Korea

dehydrocyclization of n-paraffins to aromatics [16], hydrogenation of carboxylic acids to alcohols [17] and photo catalytic oxidation of acetone [18], and also is an effective support for MoO_3-based catalysts for hydroprocessing application [19] and for $NiSO_4$ catalyst for ethylene dimerization [20] and acid catalysis [5]. Thus, the mixed TiO_2–ZrO_2 oxide has attracted attention recently as a catalyst and as a support for various applications. However, it is considered that the various binary oxides, TiO_2–ZrO_2 can be prepared differently depending on the ratio of TiO_2 to ZrO_2 and that the TiO_2–ZrO_2 composition can also influence the catalytic activity for acid catalysis. Previously, we reported the effect of TiO_2–ZrO_2 composition on catalytic activity for ethylene dimerization [21], where active sites consist of low-valent nickel and an acid. Howevr, so far, the effect of TiO_2–ZrO_2 composition on the catalytic activity for acid catalysis, 2-propanol dehydration and cumene dealkylation have not been reported.

In this investi gation, TiO_2, ZrO_2, and three kinds of TiO_2–ZrO_2 binary oxide supports having different TiO_2–ZrO_2 compositions were prepared by a precipitation method and were used as supports. In this paper, the effect of TiO_2–ZrO_2 composition on the catalytic activity of supported $NiSO_4$ for acid catalysis, 2-propanol dehydration and cumene dealkylation is reported.

2 Experimental

2.1 Catalysts

The TiO_2–ZrO_2 mixed oxides (3:1, 1:1, and 1:3 molar ratios) were prepared by a coprecipitation method using ammonium hydroxide(2.7 N) as the precipitation reagent. The coprecipitate of $Ti(OH)_4$–$Zr(OH)_4$ was obtained by adding ammonium hydroxide slowly into a mixed aqueous solution of titanium tetrachloride and zirconium oxychloride [Junsei Chemical Co.] at 60 °C with stirring until the pH of mother liquor reached about 8. The precipitates of $Ti(OH)_4$ and $Zr(OH)_4$ were obtained by adding aqueous ammonium hydroxide slowly into an aqueous solution of either titamium tetrachloride or zirconium oxychloride at room temperature with stirring. The coprecipitate and precipitates thus obtained were washed thoroughly with distilled water until chloride ions were not detected, and were dried at 100 °C for 12 h. Catalysts containing various nickel sulfate contents were prepared by dry impregnation of $Ti(OH)_4$–$Zr(OH)_4$, $Ti(OH)_4$, and $Zr(OH)_4$ powders with an aqueous solution of $NiSO_4 \cdot 6H_2O$, followed by calcining at different temperatures for 1.5 h in air. This series of catalysts is denoted by the weight % of nickel sulfate and mol % of TiO_2. For example, 20-$NiSO_4$/50$TiO_2$50-ZrO_2indicates the catalyst containing 50 mol % of TiO_2 and 20 wt % of $NiSO_4$.

2.2 Procedure

The FTIR spectra were obtained in a heatable gas cell at room temperature using a Mattson Model GL6030E spectrophotometer. The self-supporting catalyst wafers contained about 9 mg cm^{-2}. Prior to obtaining the spectra, we heated each sample under vacuum at 25–500 °C for 1 h. Catalysts were checked in order to determine the structure of the prepared catalysts by means of a Philips X'pert-APD X-ray diffractometer, employing Ni-filtered Cu K_α radiation. DSC measurements were performed by a PL-STA model 1500H apparatus in air; the heating rate was 5 °C per minute. For each experiment 10~15 mg of sample was used.

The specific surface area was determined by applying the BET method to the adsorption of N_2 at –196 °C. Chemisorption of ammonia was also employed as a measure of the acidity of catalysts. The amount of chemisorption was determined based on the irreversible adsorption of ammonia [22–24].

2-propanol dehydration was carried out at 180 °C in a pulse micro-reactor connected to a gas chromatograph. Fresh catalyst in the reactor made of 1/4 in. stainless steel was pretreated at 400 °C for 1 h in a nitrogen atmosphere. Diethyleneglycol succinate on shimalite was used as packing material of the gas chromatograph and the column temperature for analyzing the product was 150 °C. Catalytic activity for 2-propanol dehydration was represented as mol of propylene converted from 2-propanol per gram of catalyst. Cumene dealkylation was carried out at 450 °C in the same reactor as above. Packing material for the gas chromatograph was Bentone 34 on chromosorb W and column temperature was 130 °C. Catalytic activity for cumene dealkylation was represented as mol of benzene converted from cumene per gram of catalyst. Conversions for both reactions were taken as the average of the first to sixth pulse values.

3 Results and Discussion

3.1 Infrared Spectra

In general, for the metal oxides modified with the sulfate ion followed by evacuating above 400 °C, a strong band assigned to S=O stretching frequency is commonly found in the range of 1360–1410cm^{-1} [25–27]. In a separate experiment, the infrared spectra of the three self-supported catalysts after evacuation at 500 °C for 1h were examined and the results are shown in Fig. 1. In this work, the corresponding band after evacuation at room temperature was not observed, because water molecules in the air were adsorbed on the surfaces of the catalysts (Not shown in this

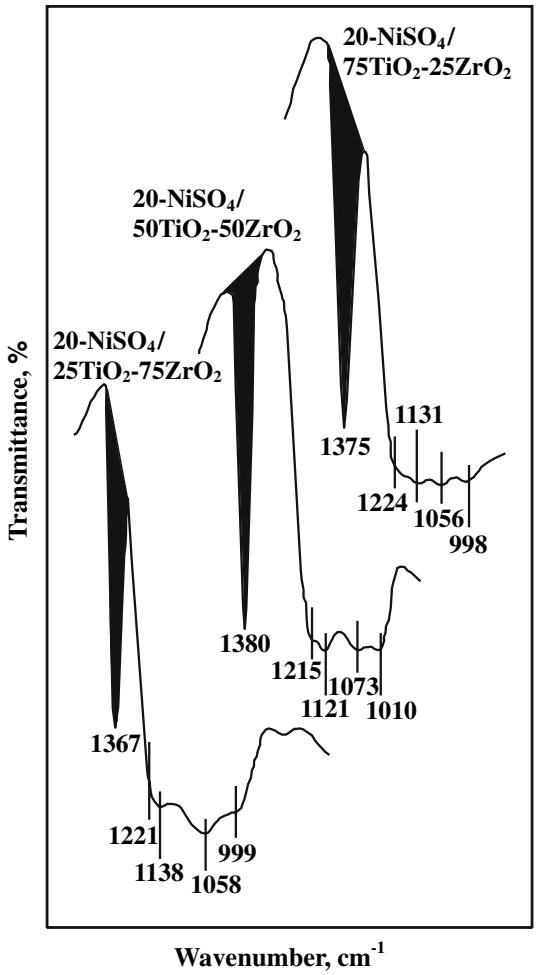

Fig. 1 Infrared spectra of 20-$NiSO_4$/25TiO_2–75ZrO_2, 20-$NiSO_4$/50TiO_2–50ZrO_2, and 20-$NiSO_4$/75TiO_2–25ZrO_2 evacuated at 500 °C for 1 h

figure). These results are very similar to those reported by other authors [26, 28, 29]. The band at 1625cm^{-1} after evacuation at room temperature is due to water molecules adsorbed on the surfaces of catalysts. As shown in Fig. 1, there are sharp and intense bands at 1367–1380 cm^{-1}, accompanied by four broad but split bands at 1224–998 cm^{-1}, indicating the presence of different sulfate species. It is likely that the surface sulfur complexes formed by the interaction of oxides with the sulfate ions in these highly active catalysts have a strong tendency to reduce their bond order by the adsorption of basic molecules, such as H_2O [25–27]. Consequently, as shown in Fig. 1, an asymmetric stretching band of S=O bonds for the sample evacuated at higher temperature appears at a higher frequency compared with that for the sample evacuated at lower temperature [25–27]. The strong ability of the sulfur complex to accommodate electrons from a basic molecule such as H_2O is a driving force in generating superacidic properties [19, 25, 27].

3.2 Structure of Catalysts

The crystalline structures of 20-$NiSO_4$/50$TiO_2$50-ZrO_2 calcined in air at different temperatures for 1.5 h were checked by X-ray diffraction. As shown in Fig. 2, for the 20-$NiSO_4$/50TiO_2–50ZrO_2 X-ray diffraction data indicated only orthorhombic phase of $ZrTiO_4$ compound at temperatures of 700 °C and above, without detection of orthorhombic $NiSO_4$ phase. Recently, Fung and Wang also reported the formation of the $ZrTiO_4$ compound at temperatures of 650 °C and above [16]. However, in a separate experiment, for pure $NiSO_4$ calcined at 800 °C a cubic phase of nickel oxide was observed due to the decomposition of nickel sulfate, showing good agreement with the results of DSC described elsewhere [30]. These results indicate that $NiSO_4$ supported on TiO_2–ZrO_2 is thermally more stable than unsupported $NiSO_4$. The other $NiSO_4$/TiO_2–ZrO_2 samples containing different $NiSO_4$ contents also exhibited results similar to that of 20-$NiSO_4$/TiO_2–ZrO_2. No diffraction line of nickel sulfate is observed at $NiSO_4$ loading up to 30 wt%, indicating good dispersion of $NiSO_4$ on the surface of TiO_2–ZrO_2 due to the interaction between them.

The 20-$NiSO_4$/25$TiO_2$75-ZrO_2 samples calcined at different temperatures are amorphous up to 600 °C (This figure not shown here). In other words, the transition

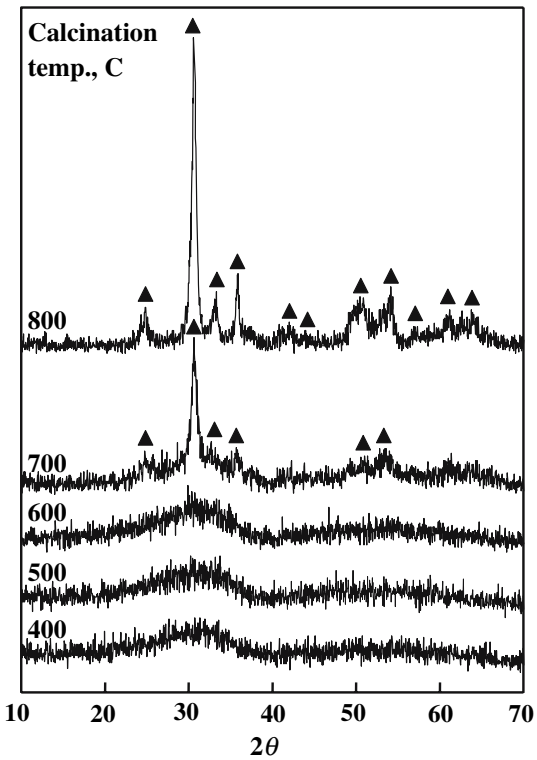

Fig. 2 X-ray diffraction patterns of 20-$NiSO_4$/50TiO_2–50ZrO_2 calcined at different temperatures: ▲, orthorhombic phase of $ZrTiO_4$

temperature of ZrO_2 from amorphous to tetragonal phase was higher by 350 °C than that of pure ZrO_2[22]. X-ray diffraction data indicated only the tetragonal phase of ZrO_2 at 700 °C, without detection of orthorhombic $NiSO_4$ phase. It is assumed that the interaction between $NiSO_4$ (or TiO_2) and ZrO_2 hinders the phase transition of ZrO_2 from amorphous to tetragonal [31]. For the above 20-$NiSO_4$/25$TiO_2$75-ZrO_2 catalyst, there are no characteristic peaks of TiO_2 in the patterns, implying that TiO_2 is sufficiently homogeneously mixed with zirconia. However, for the sample calcined at 800 °C, X-ray diffraction data indicated orthorhombic phase of $ZrTiO_4$ compound besides tetragonal phase of ZrO_2. In the case of 20 -$NiSO_4$/75$TiO_2$25-ZrO_2, TiO_2 was in the anatase phase according to XRD, showing that the amount of anatase TiO_2 phase increased upon increasing the calcination temperature. Three crystal structures of TiO_2, i.e., anatase, rutile, and brookite phases, have been reported [32, 33]. However, similarly to the results of 20-$NiSO_4$/50$TiO_2$50–ZrO_2, from 700 °C the orthorhombic phase of $ZrTiO_4$ was observed, showing that the amount of $ZrTiO_4$ increased upon increasing the calcination temperature.

3.3 Surface Properties

The thermal resistance of zirconia against sintering can be considerably improved by incorporation of a second oxide [34, 35]. As listed in Table 1, the surface area and number of acid sites of TiO_2–ZrO_2 binary oxide increased remarkably compared with the surface areas and site numbers for pure titania and zirconia. The surface area of binary oxide, 50TiO_2–50ZrO_2 is 201m^2/g, while those of single oxides, TiO_2 and ZrO_2 are 52 and 64m^2/g, respectively, showing that the surface area of binary oxide is 3–4 times higher than that of single oxide, TiO_2 or ZrO_2. It is well known that mixing two oxides can also create acidity. Tanabe's model predicts Lewis and Brönsted acid sites for mixed TiO_2–ZrO_2 [1, 14]. It has been reported that the high surface acidity of the TiO_2–ZrO_2 binary oxide is attributed to the charge imbalance based on the generation of Ti–O–Zr bonding [15]. Yu et al. have shown that TiO_2–ZrO_2 binary metal oxide exhibits higher catalytic activity

Table 1 Specific surface area and acidity of single metal oxides and binary metal oxides calcined at 500 °C for 1.5 h

Metal oxide	Surface area (m^2/g)	Acidity (μmol/g)
TiO_2	52	80
ZrO_2	64	71
25TiO_2–75ZrO_2	102	115
50TiO_2–50ZrO_2	201	168
75TiO_2–25ZrO_2	136	163

Table 2 Specific surface area of supported $NiSO_4$ catalysts calcined at 500 °C for 1.5 h

Catalyst	Surface area (m^2/g)	Acidity (μmol/g)
20-$NiSO_4$/TiO_2	74	172
20-$NiSO_4$/ZrO_2	123	215
5-$NiSO_4$/25TiO_2–75ZrO_2	109	146
20-$NiSO_4$/25TiO_2–75ZrO_2	112	261
5-$NiSO_4$/50TiO_2–50ZrO_2	271	243
20-$NiSO_4$/50TiO_2–50ZrO_2	249	356
5-$NiSO_4$/75TiO_2–25ZrO_2	232	202
20-$NiSO_4$/75TiO_2–25ZrO_2	187	320

than pure TiO_2, possibly due to an increase in surface area at a given calcination temperature and to an increase in the strength and number of acid sites [36].

It is necessary to examine the effect of nickel sulfate on the surface properties of catalysts, that is, specific surface area and acidity. The specific surface areas of 20-$NiSO_4$/25TiO_2–75ZrO_2, 20-$NiSO_4$/50TiO_2–50ZrO_2, and 20-$NiSO_4$/75TiO_2–25ZrO_2 samples are listed together with those of 20-$NiSO_4$/TiO_2 and 20-$NiSO_4$/ZrO_2 in Table 2, where all samples were calcined at 500 °C. The presence of nickel sulfate more strongly influences the surface area than is true with the supports 25TiO_2–75ZrO_2, 50TiO_2–50ZrO_2, and 75TiO_2–25ZrO_2. It is known that more active and stable catalysts can be obtained by addition of a transition metal[37–40]. It seems likely that the interactions between nickel sulfate and metal oxides prevent catalysts from crystallizating[41]. Specific surface areas of $NiSO_4$/TiO_2–ZrO_2 samples decrease gradually with increasing nickel sulfate content above 20 wt% because of the blocking of TiO_2–ZrO_2 pores by the increased $NiSO_4$ loading. The acidity increases abruptly upon the addition of nickel sulfate [5 wt% of $NiSO_4$] to TiO_2–ZrO_2, and then the acidity increases very gently with increasing nickel sulfate content up to 20 wt% for $NiSO_4$/TiO_2–ZrO_2, because of the formation of new acid sites between sulfate species and metal oxides. The surface area attained a maximum for 5-$NiSO_4$/TiO_2–ZrO_2, while the number of acid sites attained a maximum for 20-$NiSO_4$/TiO_2–ZrO_2.

Figure 3 shows the infrared spectra of ammonia adsorbed on 20-$NiSO_4$/25TiO_2–75ZrO_2, 20-$NiSO_4$/50TiO_2–50ZrO_2, and 20-$NiSO_4$/75TiO_2–25ZrO_2 samples evacuated at 500 °C for 1 h. The bands at 1453–1446 cm^{-1} on all three samples are the characteristic peaks of an ammonium ion, which are formed on the Brönsted acid sites; the absorption peaks at 1615–1612 cm^{-1} are contributed by ammonia coordinately bonded to Lewis acid sites [42, 43], indicating the presence of both Brönsted and Lewis acid sites on the surfaces of all three samples. As discussed in the infrared spectra, the intense bands at 1380–1367cm^{-1} on three

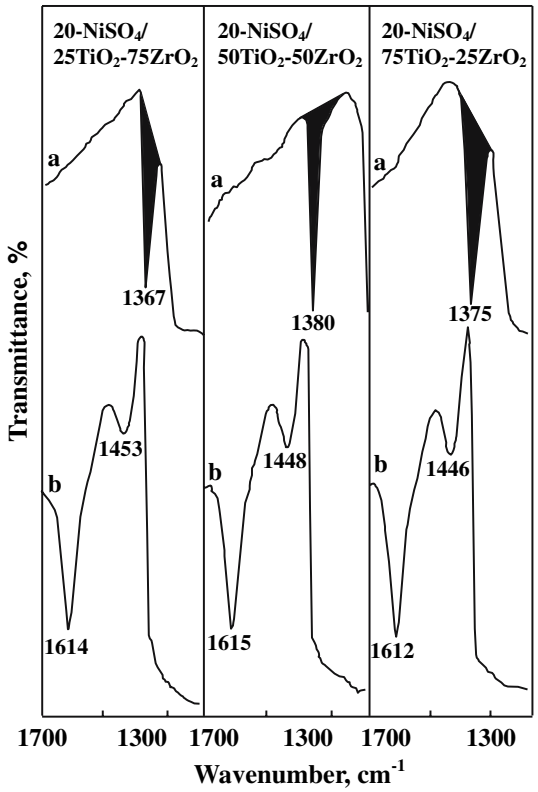

Fig. 3 Infrared spectra of NH_3 adsorbed on 20-$NiSO_4$/25TiO_2–75ZrO_2, 20-$NiSO_4$/50TiO_2–50ZrO_2, and 20-$NiSO_4$/75TiO_2–25ZrO_2: (**a**) background of catalysts after evacuation at 500 °C for 1 h, (**b**) NH_3 adsorbed on (**a**), where gas was evacuated at 230 °C for 1 h

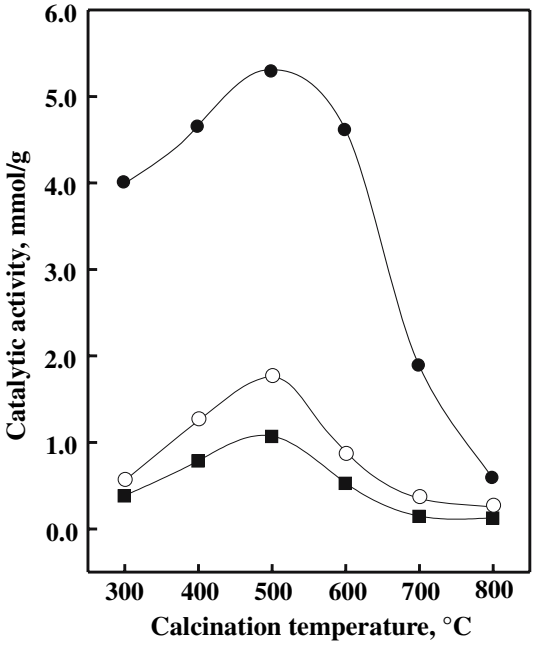

Fig. 4 Catalytic activities for 2-propanol dehydration as a function of calcination temperature: ●, 20-$NiSO_4$/50TiO_2–50ZrO_2; ○, 20-$NiSO_4$/75TiO_2–25ZrO_2; ■, 15-$NiSO_4$/25TiO_2–75ZrO_2

20-$NiSO_4$/TiO_2–ZrO_2 samples after evacuation at 500 °C are assigned to the asymmetric stretching vibration of S=O bonds having a high double bond character [26, 27, 44]. However, the drastic shift of the infrared band from 1380–1367cm^{-1} to a lower wavenumber (not shown due to the overlaps of skeletal vibration bands of TiO_2–ZrO_2) after ammonia adsorption indicates a strong interaction between an adsorbed ammonia molecules and the surface complexes. Namely, the surface sulfur compound in the highly acidic catalysts has a strong tendency to reduce the bond order of S=O from a highly covalent double-bond character to a lesser double-bond character when a basic ammonia molecule is adsorbed on the catalysts [26, 27]. Acids stronger than Ho ≤ −11.93, which corresponds to the acid strength of 100 % H_2SO_4, are considered "superacids" [26, 27]. The strong ability of the sulfur complex to accommodate electrons from a basic molecule such as ammonia is indirectly related to the driving force to generate "superacidic" properties [26, 27]. Consequently, $NiSO_4$/TiO_2–ZrO_2 catalysts would be solid "superacids", in analogy with the case of metal oxides modified with sulfate groups [25–28]. This "superacidic" property is attributable to the double bond nature of the S=O in the complex formed by the interaction between $NiSO_4$ and TiO_2–ZrO_2 [25–28].

3.4 Catalytic Activities for Acid Catalysis

3.4.1 Effect of Calcination Temperature on Catalytic Activities

Catalytic activities for 2-propanol dehydration are plotted as a function of calcination temperature in Fig. 4. The activities for three catalysts, 15-$NiSO_4$/25TiO_2–75ZrO_2, 20-$NiSO_4$/50TiO_2–50ZrO_2, and 20$NiSO_4$/75TiO_2–25ZrO_2 increased with the calcination temperature, reaching a maximum at 500 °C, and then the activities decreased. The decrease of activities for three catalysts above 500 °C can be attributed to the fact that the surface area and acidity above 500 °C decrease with the calcination temperature. In fact, both surface area and acidity of 20-$NiSO_4$/TiO_2–ZrO_2 above 500 °C were found to be decreased with the calcination temperature.

Catalytic activities for cumene dealkylation are plotted as a fuction of calcination temperature in Fig. 5. The activities for three catalysts also increased with calcination temperature, reaching a maximum at 500 °C, and then the activities decreased. Thus, hereafter, emphasis is placed only on the catalysts calcined at 500 °C. The decreases of the surface area and acidity above 500 °C can be explained in terms of that the crystalline $ZrTiO_4$ through the reaction between ZrO_2 and TiO_2 is formed. As shown in Fig. 2, the amount of crystalline $ZrTiO_4$ increased with the calcination temperature. Simultaneously, both the surface area and acidity decreased with the calcination temperature. For

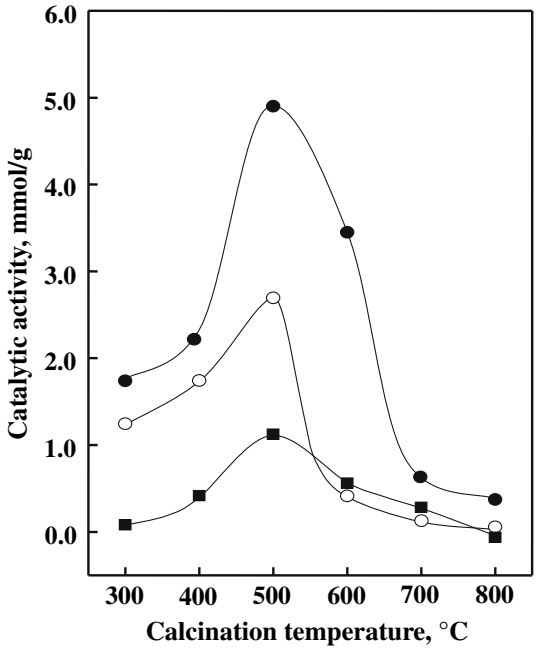

Fig. 5 Catalytic activities for cumene dealkylation as a function of calcinations temperature: ●, 20-$NiSO_4/50TiO_2$–$50ZrO_2$; ○, 20-$NiSO_4/75TiO_2$–$25ZrO_2$; ■, 25-$NiSO_4/25TiO_2$–$75ZrO_2$

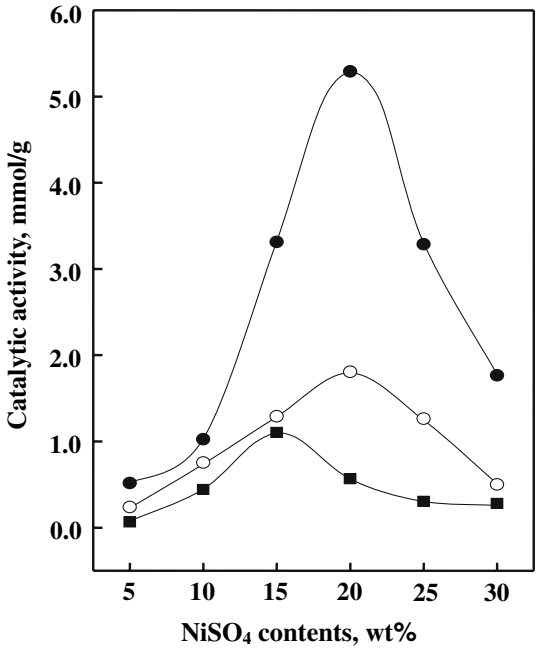

Fig. 6 Catalytic activities for 2-propanol dehydration as a function of $NiSO_4$ content: ●, $NiSO_4/50TiO_2$–$50ZrO_2$; ○, $NiSO_4/75TiO_2$–ZrO_2; ■, $NiSO_4/25TiO_2$–$75ZrO_2$

example, the surface area of 20-$NiSO_4/50TiO_2$–$50ZrO_2$ calcined at 500, 600, and 700 °C was 325, 154, and 76m^2/g, respectively. Also, the acidity of same catalysts calcined at above temperatures was 356, 308, and 130 μmol/g, respectively.

3.4.2 Effect of $NiSO_4$ Content on Catalytic Activities

It is interesting to examine how catalytic activity of acid catalyst depends on the acid property. The catalytic activity for the 2-propanol dehydration was measured; the results are illustrated as a function of $NiSO_4$ content in Fig. 6, where the reaction temperature is 180 °C. In view of Table 3 and Fig. 6, the variation in catalytic activity for 2-propanol dehydration can be roughly correlated with the changes of their acid amount, showing the highest activity and acidity for $NiSO_4/TiO_2$-ZrO_2 containing 15–20% $NiSO_4$. It has been known that 2-propanol dehydration takes place very readily on weak acid sites [5, 45]. Good correlations have been found in many cases between the acidity and the catalytic activities of solid acids. For example, the rates of both the catalytic decomposition of cumene and the polymerization of propylene over SiO_2–Al_2O_3 catalysts were found to increase with increasing acid amounts at strength $H_0 \leq +3.3$ [46]. It was also reported that the catalytic activity of nickel silicates in the ethylene demerization as well as in the butene isomerization was closely correlated with the acid amount of the catalyst [47, 48].

Cumene dealkylation takes place on relatively strong acid sites of the catalysts [45, 49, 50]. Catalytic activities for cumene dealkylation against $NiSO_4$ content are presented in Fig. 7, where reaction temperature is 450 °C. It is confirmed that the catalytic activity gives a maximum at 20–25 wt% of $NiSO_4$. This seems to be closely correlated to the specific surface area and acidity of catalysts. As listed in Table 3, the acidity attained a maximum extent when the $NiSO_4$ content in the catalyst was 15–20 wt% and then showed a gradual decrease with increasing $NiSO_4$ content. The correlation between catalytic activity and acidity holds for both reactions, 2-propanol dehydration and cumene dealkylation, although the acid strength required to catalyze acid reaction is different depending on the type of reactions. As seen in Figs. 6 and 7, the catalytic activity for cumene dealkylation, in spite of higher reaction temperature, is lower than that for 2-propanol dehydration.

3.4.3 Effect of TiO_2–ZrO_2 Composition on Catalytic Activity

Binary metal oxides are well-known in the catalysis field. It has long been observed that most binary mixtures exhibit increased surface acidity. In fact, TiO_2–ZrO_2 displays some of the highest acidities among binary metal oxides[14]. The model proposed by Tanabe et al. [1, 14] assumes that the dopant oxides cation enters the lattice of its host oxide and retains its original coordination number. Since the dopant cation is still bonded to the same number of oxygens even

Table 3 Acidity of $NiSO_4/TiO_2$–ZrO_2 catalysts containing different $NiSO_4$ contents and calcined at 500 °C for 1.5 h.

Catalyst	$NiSO_4$ content, wt%					
	5 Acidity, μmol/g	10 Acidity, μmol/g	15 Acidity, μmol/g	20 Acidity, μmol/g	25 Acidity, μmol/g	30 Acidity, μmol/g
$NiSO_4/25TiO_2$–$75ZrO_2$	120	171	204	251	240	168
$NiSO_4/50TiO_2$–$50ZrO_2$	243	279	349	356	329	257
$NiSO_4/75TiO_2$–$25ZrO_2$	202	257	349	320	318	246

though the oxygen atoms are now of a new coordination, a charge imbalance is created. Brönsted sites (extra protons) are expected to form when the charge imbalance is negative. Lewis sites are expected to form when the charge is positive. The charge imbalance is calculated for each individual bond to the dopant cation and multiplied by the number of bonds to the cation, as illustrated in following scheme.

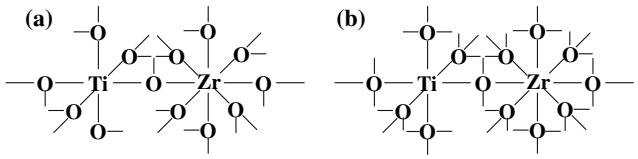

The addition of TiO_2 to ZrO_2 enhanced its acidity remarkably, showing that the acidity of $25TiO_2$–$75ZrO_2$, $50TiO_2$–$50ZrO_2$, and $75TiO_2$–$25ZrO_2$ is about 2 times as high as that of TiO_2 or ZrO_2 (Table 1). As listed in Table 2, the addition of $NiSO_4$ to TiO_2–ZrO_2 also caused the acidity of $NiSO_4/TiO_2$–ZrO_2 to increase considerably compared to TiO_2–ZrO_2, because the addition of $NiSO_4$ to TiO_2–ZrO_2 generates new acid sites by the inductive effect of sulfate species bonded to TiO_2–ZrO_2 [1, 30, 44]. Namely, the number of acid sites for 20-$NiSO_4/TiO_2$ and 20-$NiSO_4/ZrO_2$ is 172 and 215 μmol/g, respectively, while that of acid sites for 20-$NiSO_4/25TiO_2$–$75ZrO_2$, 20-$NiSO_4/50TiO_250$-ZrO_2, and 20-$NiSO_4/75TiO_2$–$25ZrO_2$ is 261, 356, and 320 μmol/g, respectively, showing a maximum acidity for 20-$NiSO_4/50TiO_250$–ZrO_2.

We examined the effect of TiO_2–ZrO_2 composition on the catalytic activity for acid catalysis. The catalytic activities for 20-$NiSO_4/TiO_2$–ZrO_2 catalysts are plotted as a function of TiO_2–ZrO_2 composition in Fig. 8. It is clear that the catalytic activities of three $NiSO_4$ catalysts supported on binary oxide TiO_2–ZrO_2 are remarkably higher than those of $NiSO_4$ catalysts supported on single oxide, TiO_2 or ZrO_2. This can be rationalized in terms of that the

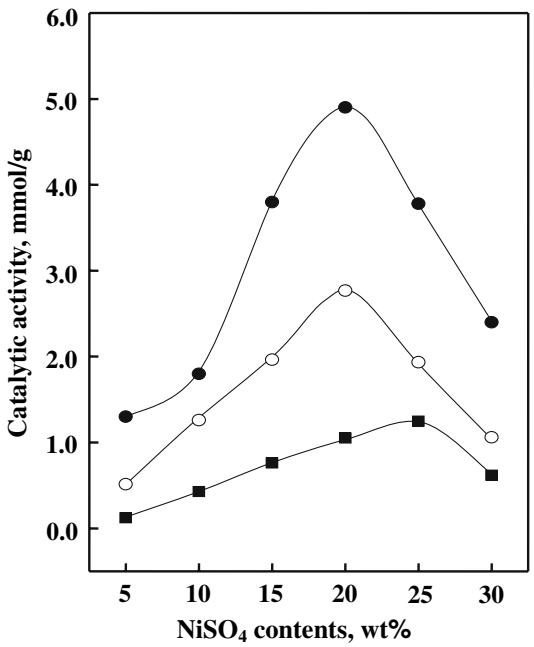

Fig. 7 Catalytic activities for cumene dealkylation as a function of $NiSO_4$ content: ●, $NiSO_4/50TiO_2$–$50ZrO_2$; ○, $NiSO_4/75TiO_2$–ZrO_2; ■, $NiSO_4/25TiO_2$–$75ZrO_2$

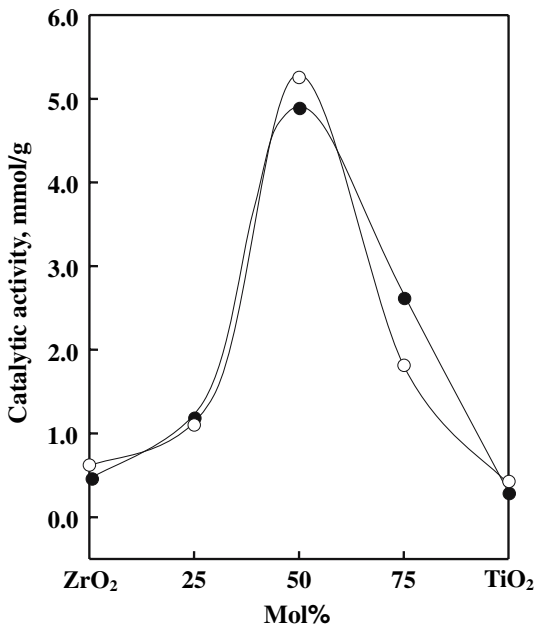

Fig. 8 Variations of catalytic activities for 2-propanol dehydration (○) and cumene dealkylation (●) with TiO_2 content

number of acid sites of TiO_2–ZrO_2 supported catalysts, 20-$NiSO_4$/TiO_2–ZrO_2 is considerably larger than that of TiO_2 or ZrO_2 supported catalyst, 20-$NiSO_4$/TiO_2 or 20-$NiSO_4$/ZrO_2, as seen in Table 2. It has been reported that the catalytic activity for acid catalysis is closely correlated with the acidity of the catalyst [3, 5, 46–48]. Therefore, it is concluded that the effect of TiO_2–ZrO_2 composition is related to an increase in the number of surface acidic sites and to the increased surface area of TiO_2–ZrO_2 supported catalysts. Within supported $NiSO_4$ catalysts, the catalytic activity for acid catalysis, 2-propanol dehydration and cumene dealkylation is in the order: 20-$NiSO_4$/50$TiO_2$50-ZrO_2 > 20-$NiSO_4$/75$TiO_2$25-ZrO_2 > 20-$NiSO_4$/25$TiO_2$75-ZrO_2 > 20-$NiSO_4$/ZrO_2 > 20-$NiSO_4$/TiO_2

4 Conclusions

A series of catalysts, $NiSO_4$/TiO_2–ZrO_2 having different TiO_2–ZrO_2 composition, for acid catalysis was prepared by the impregnation method using an aqueous solution of nickel sulfate. We examined the effect of TiO_2–ZrO_2 composition on the catalytic activity for acid catalysis, 2-propanol dehydration and cumene dealkylation. The addition of TiO_2 to ZrO_2 improved the surface area of the catalyst and increased the number of acid sites on the surface of the catalyst due to the charge imbalance of Ti–O–Zr bonding. Consequently, $NiSO_4$ supported on binary oxide, TiO_2–ZrO_2 exhibited remarkably higher catalytic activity for acid catalysis compared to $NiSO_4$ supported on single oxide, TiO_2 or ZrO_2. Within supported $NiSO_4$ catalysts, the catalytic activity for acid catalysis, 2-propanol dehydration and cumene dealkylation is in the order: 20-$NiSO_4$/50$TiO_2$50-ZrO_2 > 20-$NiSO_4$/75$TiO_2$25-ZrO_2 > 20-$NiSO_4$/25$TiO_2$75-ZrO_2 > 20-$NiSO_4$/ZrO_2 > 20-$NiSO_4$/TiO_2. The correlation between catalytic activity and acidity held for both reaction, 2-propanol dehydration and cumene dealkylation, although the acid strength required to catalyze acid reaction is different depending on the type of reactions.

Acknowledgments We wish to thank Korea Basic Science Institute (Daegu Branch) for the use of X-ray diffractometer.

References

1. Tanabe K, Misono M, Ono Y, Hattori H (1989) New solid acids and bases. Kodansha-Elsevier, Tokyo, p 185
2. Arata K (1990) Adv Catal 37:165
3. Sohn JR, Lim JS (2006) Catal Letts 108:71
4. Olah GA, Prakash GKS, Sommer J (1985) Superacids. Wiley-Interscience, New York, USA, pp 33–52
5. Sohn JR, Lee SH (2004) Appl Catal A: Gen 266:89
6. Bosman HJM, Kruissink EC, van der Spoel J, van der Brink F (1994) J Catal 148:660
7. Davis RJ, Liu Z (1997) Chem Mater 9:2311
8. Sohn JR, Jang HJ (1991) J Catal 132:563
9. Doh IJ, Pae YI, Sohn JR (1991) J Ind Eng Chem 5:161
10. Fung J, Wang I (1996) J Catal 164:166
11. Maksimov GM, Fedotov MA, Bogdanov SV, Litvak GS, Golovin AV, Likholobov VA (2000) J Mol Catal A: Chemical 158:435
12. Contescu C, Popa VT, Miller JB, Ko EI, Schwarz JA (1996) Chem Eng J 64:265
13. Scheithauer M, Grasselli RK, Knözinger H (1998) Langmuir 14:3019
14. Tanabe K, Sumiyoshi T, Shibata K, Kiyoura T, Kitagawa J (1974) Bull Chem Soc Jpn 47:1064
15. Wu JC, Chung CS, Ay CL, Wang I (1984) J Catal 87:98
16. Fung J, Wang F (1991) J Catal 130:577
17. Reddy EP, Rojas TC, Fernández A (2000) Langmuir 16:4217
18. Zorn ME, Tompkins DT, Zeltner WA, Anderson MA (1999) Appl Catal B: Environ 23:1
19. Miciukiewicz J, Mang T, Knözinger H (1995) Appl Catal A: Gen 122:151
20. Pae YI, Lee SH, Sohn JR (2005) Catal Lett 99:241
21. Sohn JR, Lee SH (2007) Appl Catal A : Gen 321:27
22. Sohn JR, Park WC (2002) Appl Catal A : Gen 230:11
23. Sohn JR, Cho SG, Pae YI, Hayashi S (1996) J Catal 159:170
24. Sohn JR, Seo DH, Lee SH (2004) J Ind Eng Chem 10:309
25. Sohn JR, Park WC, Kim HW (2002) J Catal 209:69
26. Yamaguchi T (1990) Appl Catal 61:1
27. Jin T, Yamaguchi T, Tananbe K (1986) J Phys Chem 90:4794
28. Saur O, Bensitel M, Saad ABM, Lavalley JC, Tripp CP, Morrow BA (1986) J Catal 99:104
29. Morrow BA, McFarlane RA, Lion M, Lavalley JC (1987) J Catal 107:232
30. Sohn JR, Cho ES (2005) Appl Catal A: Gen 282:147
31. Hua W, Xia Y, Yue Y, Gao Z (2000) J Catal 196:104
32. Alemany LJ, Berti F, Busca G, Ramis G, Robba D, Toledo GP, Trombetta M (1996) Appl Catal B: Environ 10:299
33. Sohn JR, Kim HW, Lim JS (2006) J Ind Eng Chem 12:104
34. Mercera PDL, van Ommen JG, Doesburg EBM, Burggraaf AJ, Ross JRH (1990) Appl Catal 57:127
35. Sohn JR, Ryu SG (1993) Langmuir 9:126
36. Yu JC, Lin J, Kwok RWM (1998) J Phys Chem B 102:5094
37. Sohn JR, Han JS (2005) J Ind Eng Chem 11:439
38. Ebitani K, Konishi J, Hattori H (1991) J Catal 130:257
39. Adeeva V, Lei GD, Sachtler WMH (1994) Appl Catal A: Gen 118:L11–L15
40. Lin CH, Hsu CY (1992) J Chem Soc Chem Commun 1479
41 Sohn JR (2004) J Ind Eng Chem 10:1
42. Basila MR, Kantner TR (1967) J Phys Chem 70:467
43. Satsuma A, Hattori A, Mizutani K, Furuta A, Miyamoto A, Hattori T, Murakami Y (1988) J Phys Chem 92:6052
44. Sohn JR, Park WC (2003) Appl Catal A: Gen 239:269
45. Decanio SJ, Sohn JR, Fritz PO, Lunsford JH (1986) J Catal 101:132
46. Tanabe K (1970) Solid acids and bases. Kodansha, Tokyo, p 103
47. Sohn JR, Ozaki A (1980) J Catal 61:291
48. Sohn JR, Park WC (2003) Appl Catal A: Gen 239:269
49. Sohn JR, Kim JG, Kwon TD, Park EH (2002) Langmuir 18:1666
50. Sohn JR, Decanio SJ, Fritz PO, Lunsford JH (1986) J Phys Chem 90:4847